

# Terrestrial Planet Finder Interferometer 2007–2008 Progress and Plans

P. R. Lawson<sup>1</sup>, O. P. Lay<sup>1</sup>, S. R. Martin<sup>1</sup>, R. D. Peters<sup>1</sup>, R. O. Gappinger<sup>1</sup>, A. Ksendzov<sup>1</sup>,  
D. P. Scharf<sup>1</sup>, A. J. Booth<sup>1</sup>, C. A. Beichman<sup>2</sup>, E. Serabyn<sup>1</sup>,  
K. J. Johnston<sup>3</sup>, W. C. Danchi<sup>4</sup>

<sup>1</sup>Jet Propulsion Laboratory, California Institute of Technology, Pasadena, CA, USA

<sup>2</sup>Michelson Science Center, California Institute of Technology, Pasadena, CA, USA

<sup>3</sup>US Naval Observatory, Washington, DC, USA

<sup>4</sup>NASA Goddard Space Flight Center, Greenbelt, MA, USA

## ABSTRACT

This paper provides an overview of technology development for the Terrestrial Planet Finder Interferometer (TPF-I). TPF-I is a mid-infrared space interferometer being designed with the capability of detecting Earth-like planets in the habitable zones around nearby stars. The overall technology roadmap is presented and progress with each of the testbeds is summarized. The current interferometer architecture, design trades, and the viability of possible reduced-scope mission concepts are also presented.

**Keywords:** Interferometry, astronomy, extrasolar planets, nulling, formation flying

## 1. INTRODUCTION AND OVERVIEW

The Terrestrial Planet Finder Interferometer (TPF-I) is a concept for a formation-flying interferometer designed to measure mid-infrared spectra of the atmospheres of Earth-like exoplanets. The primary goal of the mission is to find evidence of biological activity on planets around nearby stars. The mid-infrared provides several key biomarkers and a favorable planet-star contrast ratio. An interferometer is a compelling choice for the design of a such a mid-infrared observatory because the interferometric baselines provide unrivaled angular resolution. This is vital for unambiguous orbit determination, distinguishing multiple planets, and discrimination against structure in the exozodiacal disk. This angular resolution also provides a small inner working angle, giving access to a very broad range of target stars. In this regard, TPF-I far exceeds the predicted capability of other proposed planet-finding missions. TPF-I has been developed as a possible future collaboration between NASA and the European Space Agency (ESA).

This paper provides an update to the reviews presented at the SPIE conferences in 2006 and 2007.<sup>1,2</sup> As of September 2008, TPF will cease to exist as a NASA project in Pre-formulation Phase, but a subset of its activities will continue as pure technology development. The major achievements and/or changes in 2007–2008 have included the following:

- Completion of Milestone #1: the compensation of intensity and phase demonstrated by the Adaptive Nuller testbed. Intensity was compensated to within 0.2% and phase to within 5 nm across a 3 micron band centered at 10-microns.<sup>3,4</sup>
- Completion of Milestone #2: a demonstration of precision formation maneuvers in a ground-based robotic testbed, with performance traceability to flight.<sup>5,6</sup>
- The demonstration of nulling over a 32% bandwidth centered at a wavelength of 10 microns at a level of  $1.2 \times 10^{-5}$  using the Adaptive Nuller.<sup>4</sup>

---

Further author information: Send correspondence to Peter Lawson, Jet Propulsion Laboratory, MS 301-451, 4800 Oak Grove Drive, Pasadena CA 91109-8099, USA. E-mail: Peter.R.Lawson@jpl.nasa.gov, Telephone: +1 (818) 354-0747.

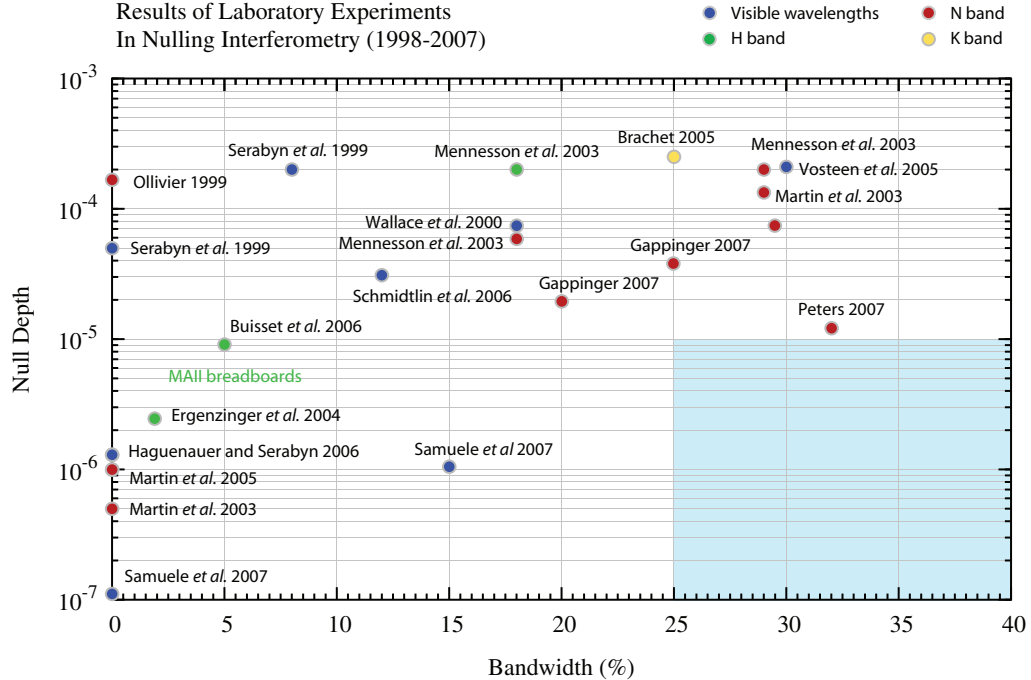


**Figure 1.** State of the Art in Nulling Interferometry: Laser experiments have shown that achromatic effects (predominantly pathlength variations) can be controlled in the lab at a level that allows nulls better than  $1 \times 10^{-6}$  to be achieved repeatedly. The best broadband nulls achieved to date have been  $1.2 \times 10^{-5}$ , with the Adaptive Nuller. The laser results therefore exceed the TPF-I requirements, and the broadband results are just shy of the TPF-I goal.

- An increased emphasis on the design of a reduced-scope mission.<sup>7</sup>
- The adoption of the Emma X-Array by both the TPF-I Project and the Darwin proposal team as the baseline mission design for TPF-I and Darwin.

All mission-specific studies ceased in 2007, and all of the testbed activities have been reduced in scope. The results of most testbed work accomplished to date has now been submitted for publication in refereed journals. In 2008 the focus of continuing work is on broadband adaptive nulling (Milestone #3) and a system-level demonstration of planet detection by four-beam array rotation with chopping and averaging (Milestone #4).

## 2. TECHNOLOGY FOR STARLIGHT SUPPRESSION

Progress in nulling interferometry is summarized in Fig. 1. The plot shows null depth as a function of bandwidth, for laboratory experiments that have been reported since 1999.<sup>8-27</sup> On the far left-hand side of the plot are shown the results obtained using lasers at visible, near-infrared, and mid-infrared wavelengths. Experiments with bandwidths as large as 40% are shown. Of principal concern to TPF-I are the experiments that have been conducted at mid-infrared wavelengths, which are indicated by the red circles in the plot. The light blue region is the performance required of TPF-I testbeds, being rejection ratios (inverse of the null depth) better than 100,000:1 with a bandwidth of 25% or larger. The reported results are almost all limited to a single-polarization input. All but one of the results are from two-beam nulling interferometers. From the results to date, we can draw the following conclusions.

1. Laser experiments have shown that achromatic effects (predominantly pathlength variations) can be controlled in the lab at a level that allows rejection ratios better than 1,000,000:1 to be achieved repeatedly. This level of performance exceeds the requirements for TPF-I. Narrow-bandwidth laser nulls have been attained with mid-infrared rejection ratios of 2,000,000:1 and at visible wavelengths of 10,000,000:1.

2. The best broad-band mid-infrared results were obtained in May 2007 with the Adaptive Nuller testbed.<sup>4</sup> A rejection ratio of 82,000:1 was obtained with a 32% bandwidth. This rejection ratio is very close to 100,000:1 and therefore almost at the level of the flight requirements. The approach used by the Adaptive Nuller is noteworthy because it is not intrinsically bandwidth limited; a spectrum is imaged onto a line of pixels on a deformable mirror to correct phase and intensity across the band, and this method can easily be extended to work well across the full 6–20  $\mu\text{m}$  science band.

If one takes into account the relaxation of requirements due to advances in our understanding of instability noise,<sup>28</sup> the best broad-band mid-infrared null have nearly demonstrated the flight requirements for TPF-I. Work is ongoing to achieve deeper nulls and to demonstrate similar capability with a four-beam testbed.<sup>29</sup>

## 2.1. Mid-IR Spatial Filter Development

Spatial filters are an essential technology for nulling interferometry. They significantly reduce the optical aberrations in wavefronts, making extremely deep nulls possible. The most basic form of a spatial filter is a simple pinhole, and pinholes have indeed been used to achieve the deepest laser nulls so far at mid-infrared wavelengths. However, pinholes only operate well over a narrow bandwidth and so are ill-suited for broadband spatial filtering for science instruments. In addition, they do not reject very low spatial-frequency wavefront aberrations. The development of improved broadband techniques for spatial filtering at mid-infrared wavelengths may be crucial to the success of TPF-I, and has been a focus of research at JPL. Although fiber optics at near-infrared wavelengths are extensively used by the telecommunications industry, low-loss, mid-IR, single-mode spatial filters are not yet commercially available. The goal of this work has been to develop single-mode spatial filters with a throughput of 50% or better with a modal suppression of 25 dB for non-fundamental modes.

### 2.1.1. Description of Research

Spatial filters may be implemented in a variety of ways, including single-mode fiber-optics made from chalcogenide or silver halide glasses, metallized waveguide structures micro-machined in silicon, or through the use of photonic crystal fibers. By promoting the parallel development of various spatial filter technologies, it was hoped that we would demonstrate the necessary spatial filter performance in the 6–20  $\mu\text{m}$  spectrum using no more than two technology types. The development of mid-infrared spatial filters was funded by TPF-I from 2003 through 2008. The performance of the single-mode filters that were developed under contract with TPF-I were tested and characterized in-house at JPL. The scope of the work included prototypes of hollow waveguide filters designed by Christopher Walker at the University of Arizona; completed chalcogenide fibers designed by Dr. Jas Sanghera at the Naval Research Laboratory (NRL); and completed silver halide fibers designed by Prof. Abraham Katzir at Tel Aviv University (TAU) in Israel.

### 2.1.2. Results

The results of this research have been published by Ksendzov et al.<sup>30,31</sup> The fibers that have been developed for TPF-I represent the state of the art. About 16 mid-infrared single-mode fibers were delivered and tested at JPL, showing excellent single-mode behavior at 10  $\mu\text{m}$ .

The 20-cm-long chalcogenide fibers developed by the Naval Research Laboratory were shown to demonstrate 30 dB rejection (a factor of 1000) of higher order modes and have an efficiency of 40%, accounting for both throughput and Fresnel losses. The transmission losses were measured at 8 dB/m, and the fibers are usable up to a wavelength of about 11  $\mu\text{m}$ . The chalcogenide fibers developed at the Naval Research Laboratory were used in the Achromatic Nulling Testbed and continue to be used in the Adaptive Nuller testbed (see Fig. 5).

The 10–20 cm long silver halide fibers that were developed by Tel Aviv University were shown to demonstrate 42 dB rejection (a factor of 16,000) of higher order modes with transmission losses of 12 dB/m. This high rejection of higher-order modes was accomplished with the addition of aperturing of the output of the fibers, made possible by the physically large diameter of the fiber cladding. Silver halide fibers should in principle be usable up to a wavelength of about 18 microns, although the laboratory tests at JPL were conducted only at 10 microns. This is the first time silver halide fibers were shown to have single-mode behavior.

### 2.1.3. Timeline

Work on hollow waveguides, begun in 2003, ceased in 2005, when it became apparent that single-mode fibers would be the most viable technology to support. The contract work with the Naval Research Laboratory on Chalcogenide fibers was successfully completed in 2005. Work up until 2007 then focused on maturing the technology for Silver Halide fibers, which was likewise successful, and work was then suspended.

### 2.1.4. Future Technology Development

An important step in future work will be to demonstrate single-mode performance over the entire wavelength band that TPF-I will use (6–20 microns). To date, experiments that test single-mode behavior have been limited to a narrow wavelength range near 10  $\mu\text{m}$ . It would be extremely useful to verify and validate the short-wavelength performance of the chalcogenide fibers and the long-wavelength performance of silver-halide fibers. Although the fibers that were developed worked very well, their throughput was not as good as one might desire for a flight mission. The spatial filtering capabilities of photonic crystal fibers should also be investigated for use at mid-infrared wavelengths, because of the improved throughput that they may provide; higher fiber throughput would effectively allow smaller collector spacecraft to be used. Also, at some future date, the suitability of these fibers for use in a cryogenic environment should be tested.

## 2.2. Achromatic Phase Shifter Studies

The Achromatic Nulling Testbed (ANT) was developed to study achromatic phase shifting techniques to achieve, broadband, dual-polarization, two-beam mid-infrared nulls. The two-beam nuller is the basic building block of all flight architectures that have been considered. Three approaches to achromatic phase shifting were investigated, with the aim of demonstrating, through one of the approaches, two-beam nulling to a level of 1 part in 100,000 with a 25% bandwidth in the 6–20  $\mu\text{m}$  range. A longer-term objective was the development of a cryogenic nulling interferometer that would meet the above requirements while operating at 40 K.

### 2.2.1. Testbed Description

Three different methods of implementing achromatic phase shifts were investigated: (1) pairs of dispersive glass plates to introduce a wavelength-dependent delay; (2) A through-focus field-flip of the light in one arm of the interferometer; and (3) successive and opposing field-reversals on reflection off flat mirrors in a periscope arrangement. A close-up view of the periscope mirrors is shown in Fig. 2. These methods were tested in the same lab, on adjacent optical benches, using a common mid-infrared laser and white-light source. The overall strategy was to develop an error budget for each approach, model the optics, isolate and measure the contributing noise sources, and compare the achievable null depths with the model predictions.

The optical breadboards were vibrationally isolated from the optical table that they were mounted on, and the table itself was further isolated from the floor. Pathlength fluctuations were monitored and maintained at a level of less than a few nanometers. The Achromatic Nulling Testbed used laser metrology and automated alignment algorithms to scan across the zero path-difference position and locate the interference null. Pathlength dither algorithms were used to locate the null and maintain the stability of the fringes.

In each of the approaches that were considered, an achromatic phase shifts of 180 degrees should be straightforward to accomplish, however in the field-reversal approaches, (2) and (3) above, a pupil-dependent polarization and/or amplitude mismatch can occur, which must then be corrected using spatial filters. Mid-infrared single-mode fibers, described previously, were therefore used with these approaches.

Ancillary optical components and detectors were developed for the Achromatic Nulling Testbed. A new high-flux continuum argon arc lamp was built to increase the dynamic range of the measurements. A view of the recombining optics, showing the intensity-balancing cross-hairs, is given in Fig. 3. Work was also undertaken to improve the low-light level limit of measurements through the development of a 10- $\mu\text{m}$  camera with high dynamic range. Components for the balancing of intensities and phases were also tested. Moreover, as noted previously, new single-mode fibers made from chalcogenide glass were used.

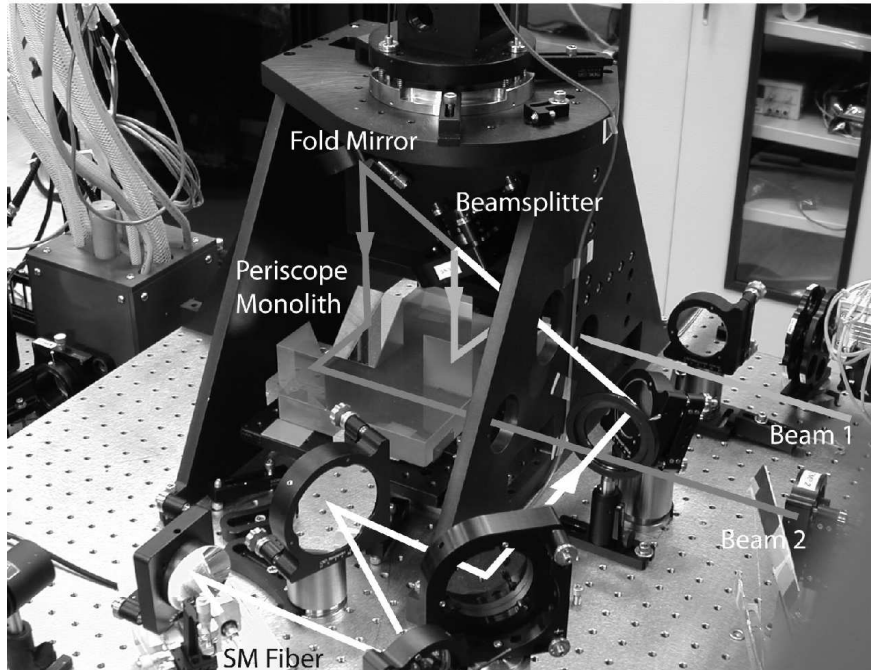


**Figure 2.** The Achromatic Nulling Testbed (ANT). The ANT included three testbeds to explore technology for achromatic phase shifters in the mid-infrared. The goal of the testbeds were to achieve mid-infrared null depths of 1000,000:1 using a bandwidth of 25%, centered at a wavelength near  $10\ \mu\text{m}$ . The view of the ANT in the above photo shows the periscope assembly. With this approach, mid-infrared nulls of 51,000:1 were achieved in polarized light with a 20% bandwidth.

### 2.2.2. Results

The results of this work have been summarized by Gappinger et al.<sup>32</sup> The most successful approach was the use of periscope mirrors, yielding an average rejection ratio of 51,000:1 at 20% bandwidth and 27,000:1 using a 25% bandwidth. The through-focus approach yielded a rejection ratio of 2000:1 with a 17% bandwidth. Pairs of glass plates provided a rejection ratio of 10,000:1 with a 25% bandwidth.

Tests using the same optics, but with narrow-band 10-m laser light and mid-infrared polarizers routinely yielded null depths of 200,000:1. The laser nulling results suggested that a factor of 4 improvement in broadband nulling was possible. There were undoubtedly wavelength-dependent effects that were different in one arm of the interferometer than in the other that limited the overall performance, although the source of these effects was never satisfactorily identified.

### 2.2.3. Timeline

The Achromatic Nulling Testbed began operations in 2003. By 2005 it had explored both the through-focus approach and the use of pairs of dispersive glass plates. From 2005 through 2007 the effort focused on developing and improving the results from the periscope mirror design. However, in May 2007 the Adaptive Nuller demonstrated deeper and more broadband nulls than could be achieved with the ANT (yielding rejection ratios of 82,000:1 over a 32% bandwidth). It seemed clear that the best approach to achromatic phase shifting was through adaptive nulling, and so the operation of the ANT was brought to a close in December 2007. The testbed was dismantled in January 2008.

### 2.2.4. Future Technology Development

Of the methods of achromatic phase shifting that were tested by the ANT, the approach using the periscope mirrors produced the best results. Although these results fell short of the goal of 100,000:1 at 25% bandwidth, this goal appears to be well within reach of the Adaptive Nuller. An adaptive nuller used in conjunction with a



**Figure 3.** Close up of the beam-combiner of the Achromatic Nulling Testbed, configured for the periscope nuller. The periscope assembly can be seen to the top right. This view includes the compensating plates and the cross-wires for intensity balancing.

periscope phase shifter would appear to be a viable approach, although it is entirely possible that an adaptive nuller alone may be sufficient. Future developments in broadband mid-infrared nulling are now being devoted to improving the performance of the adaptive nulling.

### 2.3. Adaptive Nulling

The Adaptive Nuller was designed to correct phase and intensity variations as a function of wavelength, in each of two linear polarizations. This should allow high performance nulling interferometry, while at the same time substantially relaxing the requirements on the nulling interferometer's optical components. The goal of the testbed was to demonstrate the correction of the intensity difference across the band of 8–12 microns to less than 0.2% rms ( $1 \sigma$ ) between the interferometer's arms, and at the same time correct the phase difference across the band to  $< 5 \text{ nm}$  rms ( $1 \sigma$ ). This overall correction is consistent with a null depth of  $10^{-5}$  (1 part in 100,000) if all other sources of null degradation can be neglected.

#### 2.3.1. Testbed Description

The adaptive nuller uses a deformable mirror to adjust amplitude and phase independently in each of about 12 spectral channels. The incident beam is first split into its two linear polarization components, and is dispersed into roughly a dozen spectral channels. The dispersed spectra are then imaged onto a line of pixels on a deformable mirror, so that the piston of each pixel independently adjusts the phase of each channel. Tilt in the orthogonal direction is independently adjusted, which shears the output pupil at that wavelength; this shear, in combination with an output stop, selectively reduces the intensity in that channel. The various component beams are recombined to yield an output beam that has been carefully tuned for intensity and phase in each polarization as a function of wavelength. Optical components then need only be of sufficient quality that the two arms of the interferometer are matched in intensity and phase to within the capture range of the Adaptive Nuller. A photograph of the testbed is shown in Fig. 4.

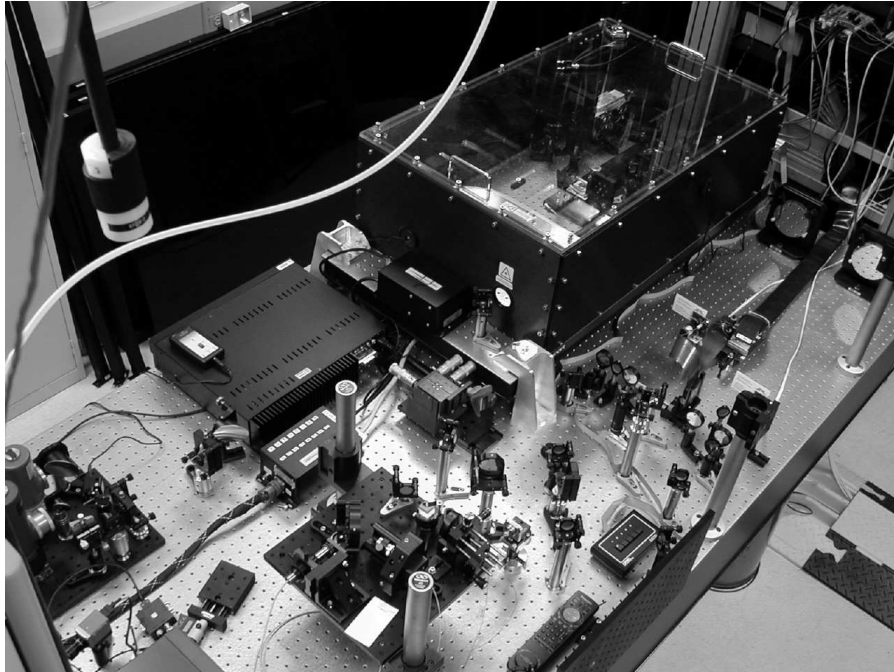


**Figure 4.** The Adaptive Nuller Testbed (AdN). The Adaptive Nuller has as its goal to demonstrate phase and intensity compensation of beams within a nulling interferometer to a level of 0.12% in amplitude and 5 nm in phase. This version of the AdN operates over a wavelength range of 8–12  $\mu\text{m}$ . The long-focus parabolas, used in AdN are seen on the upper right.

In its original concept, the Adaptive Nuller separates the light in each beam into two linear polarizations using Wollaston prisms. Although Wollaston prisms are included in the design, there are no Wollaston prisms in this mid-infrared testbed. The approach to these demonstrations has been that if light in one polarization can be compensated, then it would be straightforward to compensate both using the same overall approach. It is simply a matter of cost. At mid-infrared wavelengths, the only material that can be used to make a Wollaston prism is cadmium selenide (CdSe), which is an extremely expensive crystal to grow. Prior adaptive nulling experiments at visible wavelengths demonstrated the technique of separating the spectra, and so it wasn't deemed necessary to repeat at mid-infrared wavelengths.<sup>33</sup> Surprisingly, the mid-infrared tests with the adaptive nuller to date have been successful without using polarizing filters in the testbed.

### 2.3.2. Progress to Date

The results of this research up until 2007 have been published by Peters et al.<sup>4</sup> In March/April 2007, the testbed achieved its primary goal of demonstrating phase compensation to better than 5 nm rms across the 8–12 micron band and intensity compensation to better than 0.2%. The mid-infrared Adaptive Nuller has also demonstrated a null depth of  $1.2 \times 10^{-5}$ , over a bandwidth of 32%. This is the deepest broadband null ever achieved by a mid-infrared nulling interferometer, and almost attains the TPF-I flight requirement. Long term plans now include improving the attainable null depth to better than  $1.2 \times 10^{-5}$ , and the possible design of a cryogenic version of this testbed.

- “TPF-I Milestone #1 Whitepaper: Amplitude and Phase Control Demonstration,” Edited by R.D. Peters, P.R. Laws on, and O.P. Lay (Jet Propulsion Laboratory, December 2006).
- “TPF-I Milestone #1 Report: Amplitude and Phase Control Demonstration,” Edited by R.D. Peters, P.R. Lawson, and O.P. Lay, JPL Document 38839 (Jet Propulsion Laboratory, July 2007).

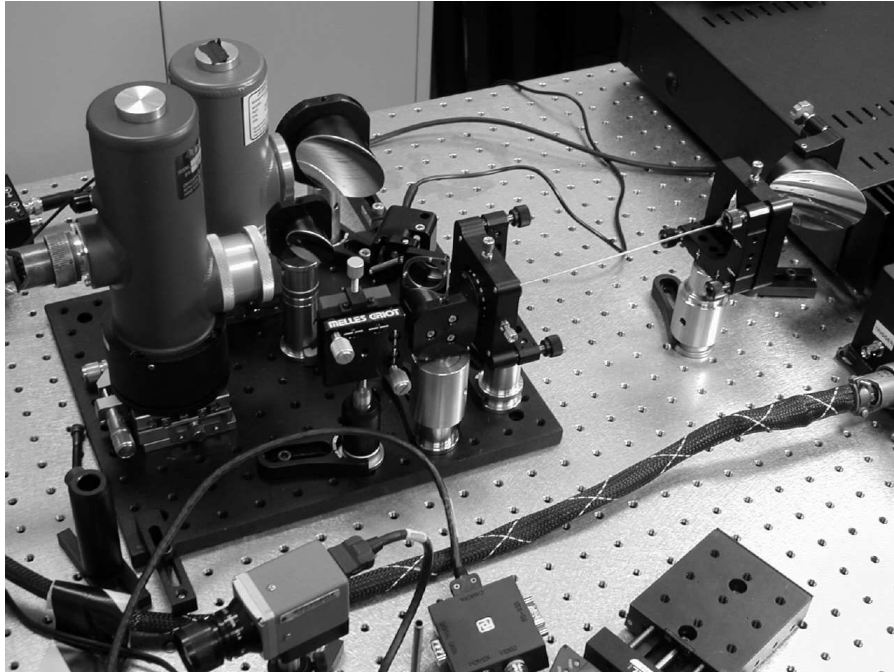


**Figure 5.** View of the back-end optics of the Adaptive Nuller testbed, showing a Chalcogenide fiber, manufactured by the US Naval Research Laboratory. The fiber is seen as a thin white line, fed by an off-axis parabola, visible toward the upper right.

- “TPF-I Milestone #3 Whitepaper: Broadband Starlight Suppression Demonstration,” Edited by P.R. Lawson, R.O. Gappinger, R.D. Peters, and O.P. Lay (Jet Propulsion Laboratory, October 2007).

## 2.4. Planet Detection Testbed

The Planet Detection Testbed, pictured in Fig. 6, was developed to demonstrate the feasibility of four-beam nulling, the achievement of the required null stability, and the consequent detection of faint planets using approaches similar to the ones contemplated for a flight-mission. The most promising architectures for a flight mission employing synthesis imaging techniques (the X-Array and the Linear Dual-Chopped Bracewell) are four-beam nulling interferometers that use interferometric chopping to detect planets in the presence of a strong mid-infrared background.

The flight mission will use a phase chopping technique to modulate a sensitivity/fringe pattern around the star. This modulation technique is in many ways similar to the use of a chopper wheel that allows the detection of infrared sources against a thermal background and/or drifting detector offsets. In this case the thermal background on the sky includes the local and exozodiacal light. To achieve this modulation the interferometer uses two nullers each phased to null out the starlight, and a second beam combiner, known as the cross-combiner, which takes the output from the nullers and phases it to form the moving sensitivity pattern. A dark null fringe is fixed over the star and the constructive bright fringes move alternately to each side of the star, thus moving on and off the planet. If there are other planets in the field of view, their signals will also contribute depending on their locations and by rotating the fringe system around the star the whole planetary system can be observed. Signal processing is then used to determine the location of the planets orbiting the star.

The primary objective of the Planet Detection Testbed is to simulate this observing scenario and demonstrate the instrument stability needed to make this process work. Stability is an important requirement of the detection process. The detected signal is the difference in the measured photon flux between the two chop states and this signal has both stochastic and systematic noise components. Integration over time reduces the stochastic



**Figure 6.** The Planet Detection Testbed (PDT). The PDT is a four-input nulling interferometer that uses  $10\ \mu\text{m}$  laser light and servo loops that modulate the null depth to perform experiments related to instability noise, interferometric chopping, and planet detection. The testbed configuration shown here was used to obtain 200,000:1 laser nulls and detect a simulated planet with a contrast ratio of 2000,000:1.

components and good instrument stability is needed to minimize systematic components which may appear as low frequency fluctuations with timescales similar to a planet signal. Some of these systematic components can be removed by signal processing using expected correlations across the broadband light spectrum. The PDT has the following main components: a star and planet source to generate a planet to be observed, a pair of nullers to null out the starlight, and a cross-combiner to allow modulation of the detected planet signal. To provide the necessary stability, the testbed has pointing and shear control systems, laser metrology systems and fringe trackers to maintain the phase on the star.

The PDT will demonstrate active control of two nulling beam combiners (four input beams in total), operated at null depths of approximately 1 part in 1 00,000 and with sufficient stability to detect a planet signal that is 1,000,000 times fainter than the simulated starlight with a signal to noise ratio of 10. This constitutes a simulation of three of the four main parts of the starlight suppression technique, deep interferometric nulling, phase chopping and formation rotation to modulate the planet.

#### **2.4.1. Testbed Description**

The Planet Detection Testbed combines four mid-infrared beams representing inputs from the four telescopes of the interferometer. In the testbed, these beams contain bright starlight and faint planet light that are separated by a pair of nullers and a phase-chopping cross combiner in a process that reproduces the operation of the flight beamcombiner. An important element of the testbed plan is to demonstrate control of the nullers and the cross-combiner at levels close to those needed for flight, and to show realistic faint planet detection within a period of about two hours in the presence of ambient laboratory noise and optical disturbances. The Planet Detection Testbed therefore includes servo loops and control systems necessary for deep and stable nulling.

An artificial star is formed from the output of a carbon dioxide laser and a small thermal source. The carbon dioxide laser light provides the 10 micron radiation which is to be nulled and the thermal source provides 2 to 4 micron radiation that is used for fringe tracking on the star. The starlight is passed through a pinhole

and chopper and then split into two beams. These beams are split again forming four beams and, at this second splitting stage, simultaneously combined with beams from a second thermal source. This second source, band-limited to radiation between 10 and 11 microns, forms the artificial planet.

System alignment, control, and calibration techniques needed for flight are being developed and tested as necessary parts of the testbed. By controlling the planet phase, the testbed will simulate a complete rotation of the telescope formation around the line of sight to the star over a 5000 s period and will demonstrate reconstruction of the planet signal from the data.

#### **2.4.2. Results**

The PDT has demonstrated 4-beam nulling using a 10 m laser with a null depth greater than 1 part in 100,000. This is one milestone towards achieving its objective of demonstrating null stability and control.

#### **2.4.3. Progress to Date**

Following successful tests in 2005, the PDT has been rebuilt to include tilt and shear sensors that in February 2007 demonstrated intensity stability in each arm of the interferometer to better than 0.2%. Experiments are underway in 2008 to achieve the principal objectives described above, and detailed in the whitepaper below:

- “Exoplanet Interferometry Milestone #4 Whitepaper: Planet Detection Demonstration,” Edited by S. R. Martin, A. J. Booth, O. P. Lay, and P. R. Lawson (Jet Propulsion Laboratory, May 2008).

### **3. TECHNOLOGY FOR FORMATION FLYING**

#### **3.1. Formation Control Testbed**

The Formation Control Testbed (FCT) was built to provide an end-to-end autonomous formation flying system in a ground-based laboratory. The FCT provides an environment for system-level demonstration and validation of formation control algorithms. The algorithms are validated using multiple floating test robots that emulate real spacecraft dynamics. The goal is to demonstrate algorithms for formation acquisition, formation maneuvering, fault-tolerant operations, as well as collision-avoidance maneuvering.

##### **3.1.1. Testbed Description**

The FCT is comprised of two robots with flight-like hardware and dynamics, a precision flat floor for the robots to operate on, ceiling-mounted artificial stars for robot attitude sensing and navigation, and a “ground control” room for commanding the robots and receiving telemetry. The robots and part of the flat floor are shown in Fig. 7. The layout of the FCT emulates the environment of a formation of telescopes that is restricted to maneuvering in the same plane in space, normal to the direction of the target star.

To be as flight-like as possible, each robot is equipped with a typical single-spacecraft attitude control suite of reaction wheels, gyros, and a star tracker. Thrusters are also available for attitude control. Each robot has a lower translational platform and an upper attitude platform. The attitude platform is the “spacecraft” and is completely disconnected from the translational platform.

\* The attitude platform/spacecraft houses the avionics, actuators, sensors, inter-robot and “ground”-to-robot wireless communication antennae, and the spacecraft processors.

\* The translational platform provides both translational and rotational degrees of freedom to the attitude platform via (i) linear air bearings (the black, circular pads at the base of each robot) that allow the entire robot to float freely on the flat floor, and (ii) a spherical air bearing at the top of the vertical stage (the black, vertical cylinders).

Each robot therefore has five degrees-of-freedom: two in translation and three in rotation. The robots can translate wherever necessary on the flat floor; however, the pitch and roll axes of each robot’s motion are limited to 30 (a physical limitation of the spherical air bearings). The formation algorithms are designed for all six degrees-of-freedom, and for the vertical translational degree of freedom, telescoping vertical stages with 0.5 m of travel are being retrofitted in 2008. The vertical air bearing will have a range of 25 cm.

The FCT is housed in the former Celestarium, which had been used to calibrate star trackers. The FCT has a 40 ft. diameter circular floor space and a 25 ft. high, dome-like ceiling. This ceiling is ideal for mounting artificial reference stars. The precision flat floor that the robots operate on is contained within the 40 ft. diameter floor space. The flat floor consists of fourteen 4 ft. x 12 ft. metal panels ground to a flatness of 0.002 in. Each panel is mounted on a support structure that has coarse and vernier leveling screws. Periodic laser surveys of the floor are used to ensure that the steps between the panels are less than 0.001 inch and the floor slope is less than 120 microradians. The resulting 7.3 m x 8.5 m flat floor is sufficient to demonstrate nominal TPF-I formation maneuvers, such as formation rotations and collision avoidance.

To provide artificial stars, down-looking infrared LEDs are mounted on the ceiling of the Celestarium. The star tracker on each robot measures the direction (two angles) to at least three stars. From this information, the attitude and position of a robot can be determined with respect to the “inertial” Room Frame. The position of a robot can also be determined because the stars are in the near-field, and hence, the direction to an LED changes as a robot moves.

### 3.1.2. Results

In 2007 the Formation Control Testbed demonstrated precision maneuvers using two robots, showing autonomous initialization, maneuvering, and operation in a collision free manner. The key maneuver that was demonstrated was representative of TPF-I science observations. Repeated experiments with the robots demonstrated formation rotations through greater than 90 at ten times the flight rotation rate while maintaining a relative position control to 5 cm rms. Although the achievable resolution in these experiments was limited by the noise environment of the laboratory, it was nonetheless demonstrated (through modeling) that in the relatively noise-free environment of space, the performance of these algorithms would exceed TPF-I flight requirements.

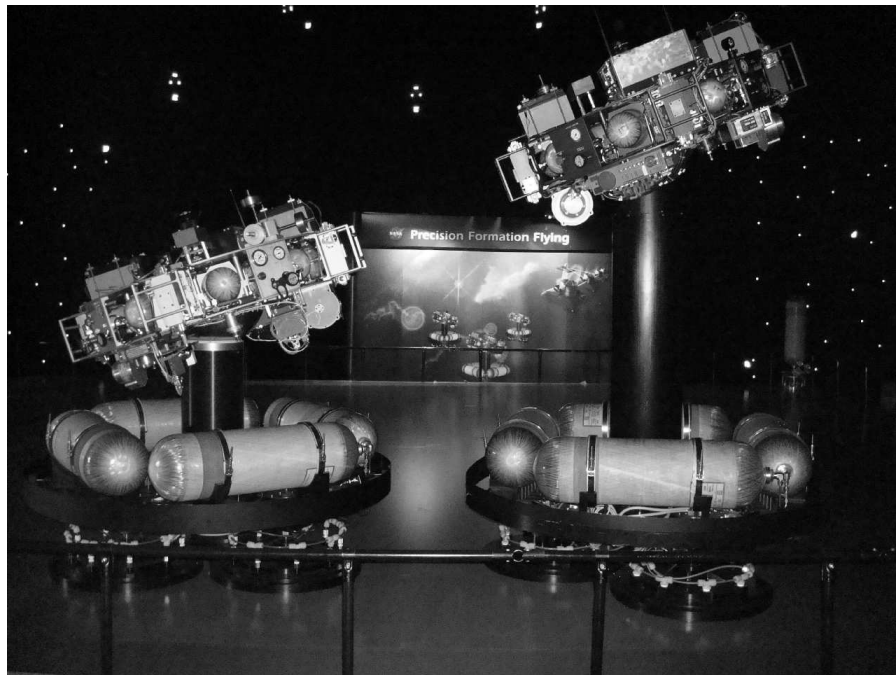


**Figure 7.** The Formation Control Testbed (FCT). Shown here are the two robots of the FCT. Each robot carries canisters of compressed air that allow them to float off a polished metal floor. The floor is flat to within 2 one-thousandths of an inch and spans a much larger area than shown here. The robots carry a platform (shown tilted for each robot) that is supported on a spherical ball bearing, also driven with compressed air so that the support of the platform is entirely frictionless. The robots serve as the hardware interface and testing ground for flight software developed for space applications in formation flying.

### 3.1.3. Timeline

Planning for the Formation Control Testbed began in 2003. The first robot for the FCT was commissioned in September 2004 and the second in January 2006. In May 2006 the integration of the FACS software was successfully completed for the robots, enabling them to operate in a formation mode for the first time. In late 2006 and early 2007 the robots underwent extensive hardware upgrades in preparation for their performance milestone, described previously. The experiments for that milestone were conducted in September 2007. In November 2007 the first vertical stage was commissioned for one of the robots. The vertical stage for the second robot is anticipated in June of 2008. The research sponsored by NASA for TPF was concluded in January 2008. The Formation Control Testbed continues to be developed in support of DARPA and its F-6 Program.

- “TPF-I Milestone #2 Whitepaper: Formation Control Performance Demonstration,” Edited by D.P. Scharf (Jet Propulsion Laboratory, May 2007).
- ‘TPF-I Milestone #2 Report: Formation Control Performance Demonstration,’ Edited by D.P. Scharf and P. R. Lawson, JPL Document 43009 (Jet Propulsion Laboratory, January 2008).

### 3.1.4. Future Technology Development

The two flight-like robots of the FCT have now demonstrated precision formation control for synchronized rotations. This is representative of the highest precision maneuver needed for TPF-I, with performance traceable to flight. The next steps for technology maturation that could be done using the robots within the FCT include demonstrating new capabilities such as (1) reactive collision avoidance, (2) formation fault detection, and (3) autonomous reconfiguration and retargeting maneuvers. Using the real-time simulation environment of FAST we would also need to demonstrate the performance with full formation-flight complexity, that is with five interacting spacecraft showing synchronized rotations, autonomous reconfigurations, fault detection, and collision avoidance. The greatest advance in maturing technology for formation flying would be to have a modest-scale technology mission devoted to verifying and validating guidance and control algorithms such as those developed through the FCT.

The European Space Agency and national space agencies in Europe have a program of precursor missions to gain experience in formation flying to support XEUS and Darwin. In 2009 the Swedish Space Agency will launch the Prisma mission. This is primarily a rendezvous and docking mission, but will also test out RF metrology designed for Darwin. In 2012 ESA plans to launch Proba-3, which is specifically a technology precursor to XEUS, and will include optical metrology loops for sub-millimeter range control over a 30-m spacecraft separation. The French and Italian space agencies are planning to launch Simbol-X in 2014. Simbol-X is an x-ray science mission with an architecture very similar to XEUS, but with a 20-m spacecraft separation. Simbol-X is to enter Phase B of development in the summer of 2008.

A ground-based facility such as the FCT provides the means to test and improve real-time formation-flying algorithms as the technology matures, even while the technology is proven in space. Although two-spacecraft precision maneuvers were demonstrated in 2007, a major goal that remains is to demonstrate robust algorithms for three or more spacecraft, such as would be used by TPF-I.

## 4. SUMMARY

Technology development for the Terrestrial Planet Finder Interferometer is proceeding well, and the technology for nulling interferometry is reaching maturity. The performance of the Adaptive Nuller has yielded null depths just shy of the flight requirements and promises to dramatically change the course of our present technology development. Both TPF-I and Darwin now have a common interferometer architecture that reduces the cost and complexity of a mid-infrared formation flying mission. However, all planet-finding missions within the Navigator Program are being reassessed prior to the 2010 Decadal Survey, because of concerns for mission lifecycle costs. Darwin/TPF-I will certainly be a very ambitious mission, and this collaboration is now under review both within NASA and at ESA as part of the *Cosmic Vision* planning.

## ACKNOWLEDGMENTS

This work was conducted at the Jet Propulsion Laboratory, California Institute of Technology, under contract with the National Aeronautics and Space Administration. Reference in this paper to any specific commercial product, process, or service by trade name, trademark, manufacturer, or otherwise, does not constitute or imply its endorsement by the United States Government or the Jet Propulsion Laboratory, California Institute of Technology.

342935363738323930314012414228434445467214734484956505152

## REFERENCES

1. P. R. Lawson, A. Ahmed, R. O. Gappinger, A. Ksendzov, O. P. Lay, S. R. Martin, R. D. Peters, D. P. Scharf, J. K. Wallace, and B. Ware, "Terrestrial Planet Finder Interferometer: Technology status and plans," in *Advances in Stellar Interferometry*, J. Monnier, M. Schöller, and W. Danchi, eds., *Proc. SPIE* **6268**, p. 626828, 2006.
2. P. R. Lawson, O. P. Lay, S. R. Martin, C. A. Beichman, K. J. Johnston, W. C. Danchi, R. O. Gappinger, S. L. Hunyadi, A. Ksendzov, B. Mennesson, R. D. Peters, D. P. Scharf, E. Serabyn, and S. C. Unwin, "Terrestrial planet finder interferometer: 2006-2007 progress and plans," in *Techniques and Instrumentation for Detection of Exoplanets III*, D. R. Coulter, ed., *Proc. SPIE* **6693**, p. 669308, 2007.
3. R. D. Peters, O. P. Lay, and M. Jeganathan, "Adaptive nulling in the mid-ir for the Terrestrial Planet Finder Interferometer," in *Techniques and Instrumentation for Detection of Exoplanets III*, D. R. Coulter, ed., *Proc. SPIE* **6693**, p. 669315, 2007.
4. R. D. Peters, O. P. Lay, and M. Jeganathan, "Broadband phase and intensity compensation with a deformable mirror for an interferometric nuller," *Appl. Opt.* **47**, p. in press, 2008.
5. D. P. Scharf, J. A. Keim, F. Y. Hadaegh, E. G. Benowitz, and P. R. Lawson, "Flight-like ground demonstration of precision formation flying spacecraft," in *Techniques and Instrumentation for Detection of Exoplanets III*, D. R. Coulter, ed., *Proc. SPIE* **6693**, p. 669307, 2007.
6. D. P. Scharf, F. Y. Hadaegh, J. A. Keim, A. C. Morfopoulos, A. Ahmed, Y. Brenman, A. Vafaei, J. F. Shields, C. F. Bergh, and P. R. Lawson, "Flight-like ground demonstrations of precision maneuvers for spacecraft formations," *AIAA Journal of Guidance, Control, and Dynamics* **31**, p. submitted, 2008.
7. S. R. Martin, "TPF-Emma: concept study of a planet finding space interferometer," in *Techniques and Instrumentation for Detection of Exoplanets III*, D. R. Coulter, ed., *Proc. SPIE* **6693**, p. 669309, 2007.
8. H. Bokhove, J. P. Kappelhof, H. J. P. Vink, L. L. A. Vosteen, and Z. Sodnik, "Broadband nulling using a prism phase shifter," in *Towards Other Earths: Darwin/TPF and the Search for Extrasolar Terrestrial Planets*, M. Fridlund and T. Henning, eds., **SP-539**, pp. 367–369, European Space Agency, (Noordwijk, The Netherlands), 2003.
9. F. Brachet, A. Labéque, A. Léger, M. Ollivier, C. L. V. Hervier, B. Chazelas, B. Pellet, T. Lépine, and C. Valette, "Nulling interferometry for the darwin mission: Polychromatic laboratory test bench," in *New Frontiers in Stellar Interferometry*, W. A. Traub, ed., *Proc. SPIE* **5491**, pp. 991–998, 2004.
10. C. B. X. Rejeaunier, Y. Rabbia, C. Ruilier, M. Barillot, L. Lierstuen, and J. M. Perdignes Armeng, "Multi-axial nulling interferometry: Demonstration of deep nulling and investigations of polarization effects," in *Advances in Stellar Interferometry*, J. D. Monnier, M. Schöller, and W. C. Danchi, eds., *Proc. SPIE* **6268**, p. 626819, 2006.
11. C. Buisset, X. Rejeaunier, Y. Rabbia, and M. Barillot, "Stable deep nulling in polychromatic unpolarized light with multi-axial beam combination," *Appl. Opt.* **46**, pp. 7817–7822, 2007.
12. K. Ergenzinger, R. Flatscher, U. Johann, R. Vink, and Z. Sodnik, "Eads astrium nulling interferometer breadboard for darwin and genie," in *Proc. Int. Conf. Space Optics*, M. Fridlund and T. Henning, eds., **SP-554**, pp. 223–230, European Space Agency, (Noordwijk, The Netherlands), 2004.
13. P. Haguenauer and E. Serabyn, "Deep nulling of laser light with a single-mode-fiber beam combiner," *Appl. Opt.* **45**, pp. 2749–2754, 2006.
14. S. R. Martin, R. O. Gappinger, F. M. Loya, B. P. Mennesson, S. L. Crawford, and E. Serabyn, "A mid-infrared nuller for the Terrestrial Planet Finder: Design, progress, and results," in *Techniques and Instrumentation for Detection of Exoplanets*, D. R. Coulter, ed., *Proc. SPIE* **5170**, pp. 144–154, 2003.

15. S. R. Martin, E. Serabyn, and G. J. Hardy, "Deep nulling of laser light in a rotational shearing interferometer," in *Interferometry for Optical Astronomy II*, W. A. Traub, ed., *Proc. SPIE* **4838**, pp. 656–667, 2003.
16. S. Martin, P. Szwaykowski, and F. Loya, "Testing exo-planet signal extraction using the Terrestrial Planet Finder Planet Detection Testbed," in *Techniques and Instrumentation for Detection of Exoplanets II*, D. R. Coulter, ed., *Proc. SPIE* **5905**, p. 590508, 2005.
17. S. Martin, "The flight instrument design for the Terrestrial Planet Finder Interferometer," in *Techniques and Instrumentation for Detection of Exoplanets II*, D. R. Coulter, ed., *Proc. SPIE* **5905**, pp. 21–35, 2005.
18. B. Mennesson, S. L. Crawford, E. Serabyn, S. Martin, M. Creech-Eakman, and G. Hardy, "Laboratory performance of the Keck Interferometer nulling beam combiner," in *Towards Other Earths: Darwin/TPF and the Search for Extrasolar Terrestrial Planets*, M. Fridlund and T. Henning, eds., **SP-539**, pp. 525–529, European Space Agency, (Noordwijk, The Netherlands), 2003.
19. B. Mennesson, P. Haguenaer, E. Serabyn, and K. Liewer, "Deep broad-band infrared nulling using a single-mode fiber beam combiner and baseline rotation," in *Advances in Stellar Interferometry*, J. D. Monnier, M. Schöller, and W. C. Danchi, eds., *Proc. SPIE* **6268**, p. 626830, 2006.
20. R. M. Morgan, J. H. Burge, and N. J. Woolf, "Final laboratory results of visible nulling with dielectric plates," in *Interferometry for Optical Astronomy II*, W. A. Traub, ed., *Proc. SPIE* **4838**, pp. 644–655, 2003.
21. M. Ollivier, *Contribution à la Recherche d'Exoplanètes: Coronagraphie Interférentielle pour la Mission Darwin*. PhD thesis, University Paris XI, Orsay, France, 1999.
22. R. Samuele, J. K. Wallace, E. Schmidtlin, M. Shao, B. M. Levine, and S. Fregoso, "Experimental progress and results of a visible nulling coronagraph," in *2007 IEEE Aerospace Conference*, p. paper 1333, 2007.
23. E. Schmidtlin, J. K. Wallace, R. Samuele, B. M. Levine, and M. Shao, "Recent progress of visible light nulling and first 1 million null result," in *Direct Imaging of Exoplanets: Science and Techniques*, C. Aime and F. Vakili, eds., *Proc. IAU Colloq.* **200**, pp. 353–360, 2006.
24. E. Serabyn, J. K. Wallace, G. J. Hardy, E. G. H. Schmidtlin, and H. T. Nguyen, "Deep nulling of visible laserlight," *Appl. Opt.* **38**, pp. 7128–7132, 1999.
25. L. L. A. Vosteen, H. J. P. Vink, H. van Brug, and H. Bokhove, "Achromatic phase-shifter breadboard extensions," in *Techniques and Instrumentation for Detection of Exoplanets II*, D. R. Coulter, ed., *Proc. SPIE* **5905**, p. 59050A, 2005.
26. J. K. Wallace, G. Hardy, and E. Serabyn, "Deep and stable interferometric nulling of broadband light with implications for observing planets around nearby stars," *Nature* **406**, pp. 700–702, 2000.
27. V. Weber, M. Barillot, P. Haguenaer, P. Kern, I. Schanen-Duport, P. Labeye, L. Pujol, and Z. Sodnik, "Nulling interferometer based on an integrated optics combiner," in *New Frontiers in Stellar Interferometry*, W. A. Traub, ed., *Proc. SPIE* **5491**, pp. 842–850, 2004.
28. O. P. Lay, "Removing instability noise in nulling interferometers," in *Advances in Stellar Interferometry*, J. D. Monnier, M. Schöller, and W. C. Danchi, eds., *Proc. SPIE* **6268**, p. 62681A, 2006.
29. A. J. Booth and S. R. Martin, "Terrestrial Planet Finder, Planet Detection Testbed: latest results of planet light detection in the presence of starlight," in *Optical and Infrared Interferometry*, M. Schöller, W. C. Danchi, and F. Delplancke, eds., *Proc. SPIE* **7013**, p. these proceedings, 2008.
30. A. Ksendzov, O. Lay, S. Martin, J. S. Sanghera, L. E. Busse, W. H. Kim, P. C. Pureza, and V. Q. Nguyen, "Characterization of mid-infrared single mode fibers as modal filters," *Appl. Opt.* **46**, pp. 7957–7962, 2007.
31. A. Ksendzov, T. Lewi, O. Lay, S. Martin, R. Gappinger, P. Lawson, R. Peters, S. Shalem, A. Tsun, and A. Katzir, "Modal filtering in mid-infrared using single mode silver halide fibers," *Appl. Opt.* **47**, p. submitted, 2008.
32. R. O. Gappinger, R. T. Diaz, P. R. Lawson, S. R. Martin, O. P. Lay, J. K. Wallace, and F. M. Loya, "Experimental evaluation of achromatic phase shifters for mid-infrared starlight suppression," *Appl. Opt.* **47**, p. submitted, 2008.
33. R. D. Peters, A. Hirai, M. Jeganathan, and O. P. Lay, "Near-ir demonstration of adaptive nuller based on deformable mirror," in *New Frontiers in Stellar Interferometry*, W. A. Traub, ed., *Proc. SPIE* **5491**, pp. 1630–1638, 2004.

34. C. A. Beichman, P. Lawson, O. Lay, A. Ahmed, S. Unwin, and K. Johnston, "Status of the Terrestrial Planet Finder Interferometer," in *Advances in Stellar Interferometry*, J. Monnier, M. Schöller, and W. Danchi, eds., *Proc. SPIE* **6268**, p. 62680S, 2006.
35. R. N. Bracewell, "Detecting nonsolar planets by spinning infrared interferometer," *Nature* **274**, p. 780, 1978.
36. C. V. M. Fridlund, L. d'Arcio, R. den Hartog, and A. Karlsson, "Status and recent progress of the Darwin mission in the Cosmic Vision program," in *Advances in Stellar Interferometry*, J. Monnier, M. Schöller, and W. Danchi, eds., *Proc. SPIE* **6268**, p. 62680R, 2006.
37. D. J. Des Marais, M. O. Harwit, K. W. Jucks, J. F. Kasting, D. N. C. Lin, J. I. Lunine, J. Schneider, S. Seager, W. A. Traub, and N. J. Woolf, "Remote sensing of planetary properties and biosignatures of extrasolar terrestrial planets," *Astrobiology* **2**, pp. 153–181, 2002.
38. R. O. Gappinger, R. T. Diaz, S. R. Martin, F. M. Loya, and P. R. Lawson, "Current progress on TPF-I achromatic nulling at the Jet Propulsion Laboratory," in *Techniques and Instrumentation for Detection of Exoplanets III*, D. R. Coulter, ed., *Proc. SPIE* **6693**, p. 669318, 2007.
39. A. Ksendzov, E. Bloemhof, V. White, J. K. Wallace, R. O. Gappinger, J. S. Sanghera, L. E. Busse, W. J. Kim, P. C. Pureza, V. Q. Nguyen, I. D. Aggarwal, S. Shalem, and A. Katzir, "Measurement of spatial filtering capabilities of single mode infrared fibers," in *Advances in Stellar Interferometry*, J. Monnier, M. Schöller, and W. Danchi, eds., *Proc. SPIE* **6268**, p. 626838, 2006.
40. P. R. Lawson and J. A. Dooley eds., *Technology Plan for the Terrestrial Planet Finder Interferometer*, Jet Propulsion Laboratory Publications, Pasadena, California, JPL Pub. 05-5, June 2005.
41. O. P. Lay and S. Dubovitsky, "Nulling interferometers: the importance of systematic errors and the X-array configuration," in *New Frontiers in Stellar Interferometry*, W. A. Traub, ed., *Proc. SPIE* **5491**, pp. 874–885, 2004.
42. O. P. Lay, S. M. Gunter, L. A. Hamlin, C. A. Henry, Y. Li, S. R. Martin, G. H. Purcell, B. Ware, J. A. Wertz, and M. C. Noecker, "Architecture trade study for the Terrestrial Planet Finder Interferometer," in *Techniques and Instrumentation for Detection of Exoplanets II*, D. R. Coulter, ed., *Proc. SPIE* **5905**, pp. 8–20, 2005.
43. O. P. Lay, S. R. Martin, and S. L. Hunyadi, "Planet-finding performance of the TPF-I Emma architecture," in *Techniques and Instrumentation for Detection of Exoplanets III*, D. R. Coulter, ed., *Proc. SPIE* **6693**, p. 66930A, 2007.
44. O. P. Lay, "Imaging properties of rotating nulling interferometers," *Appl. Opt.* **44**, pp. 5859–5871, 2005.
45. O. P. Lay, "Systematic errors in nulling interferometers," *Appl. Opt.* **43**, pp. 6100–6123, 2004.
46. S. R. Martin, P. Szwajkowski, F. M. Loya, and K. Liewer, "Progress in testing exo-planet signal extraction on the TPF-I Planet Detection Testbed," in *Advances in Stellar Interferometry*, J. Monnier, M. Schöller, and W. Danchi, eds., *Proc. SPIE* **6268**, p. 626818, 2006.
47. R. D. Peters, O. P. Lay, A. Hirai, and M. Jeganathan, "Adaptive nulling for the Terrestrial Planet Finding Interferometer," in *Advances in Stellar Interferometry*, J. Monnier, M. Schöller, and W. Danchi, eds., *Proc. SPIE* **6268**, p. 62681C, 2006.
48. R. D. Peters and O. P. Lay, "Progress in deep broadband interferometric nulling with the Adaptive Nuller," in *Optical and Infrared Interferometry*, M. Schöller, W. C. Danchi, and F. Delplancke, eds., *Proc. SPIE* **7013**, p. these proceedings, 2008.
49. C. Ruilier, R. Krawczyk, M. Sghedoni, O. Chanal, C. Degrelle, L. Pirson, O. Simane, and E. Thomas, "System assessment study of the ESA Darwin mission: concepts trade-off and first iteration design on novel emma arrangement," in *Techniques and Instrumentation for Detection of Exoplanets III*, D. R. Coulter, ed., *Proc. SPIE* **6693**, p. 66930T, 2007.
50. C. A. Beichman, N. J. Woolf, and C. A. Lindensmith eds., *The Terrestrial Planet Finder (TPF)*, Jet Propulsion Laboratory Publications, Pasadena, California, JPL Pub. 99-3, May 1999.
51. P. R. Lawson, O. P. Lay, K. J. Johnston, and C. A. Beichman, *The Terrestrial Planet Finder Science Working Group Report*, Jet Propulsion Laboratory, Pasadena, California, 2007. JPL Pub 07-1.
52. O. Wallner, K. Ergenzinger, R. Flatscher II, and U. A. Johann, "X-array aperture configuration in planar or non-planar spacecraft formation for DARWIN/TPF-I candidate architectures," in *Techniques and Instrumentation for Detection of Exoplanets III*, D. R. Coulter, ed., *Proc. SPIE* **6693**, p. 66930U, 2007.